International Journal of Religion
2025
Volume: 6| Number 1 | pp. 377 – 395
ISSN: 2633-352X (Print) | ISSN: 2633-3538 (Online)
ijor.co.uk
DOI: https://doi.org/10.61707/s51hjt17

Research on Evaluating EEG Signal Processing Methods for the Development of BCI Systems

Chau Thi Ma[1], Hieu Nguyen Dinh[2], Kien Nguyen Minh[3] and Long Vu Thanh[4]

Abstract

This article investigates the evaluation of EEG signal processing methods to enhance the development of Brain-Computer Interface (BCI) systems. Given the critical role of EEG signal quality in determining BCI performance, we explore the impact of various noise types—such as artifacts from eye movements, muscle activity, and electronic interference—on signal integrity. We focus on noise filtering techniques, particularly their effectiveness in preserving essential signal components while eliminating unwanted noise. Our research includes a detailed analysis of several common noise processing methods, including Independent Component Analysis (ICA), Discrete Wavelet Transform (DWT), and bandpass filtering. Through comprehensive testing on real EEG signals, we identify optimal strategies for improving signal quality. The findings suggest that while ICA offers high-level noise filtering, it requires expert intervention for effective implementation. In contrast, the bandpass filter demonstrates significant potential for automated noise reduction, providing stable performance with minimal computational cost. Applying these methods before classification has shown to enhance BCI system accuracy significantly. This study contributes to the ongoing efforts to refine BCI algorithms by identifying effective noise-filtering strategies that can be seamlessly integrated into practical applications.

Keywords: *EEG Signal, Brain-Computer Interface, Independent Component Analysis, Discrete Wavelet Transform, Bandpass Filter*

INTRODUCTION

In BCI systems, optimizing algorithms to enhance accuracy and efficiency is crucial. The quality of the input signal is vital for ensuring system performance; however, electroencephalogram (EEG) signals are often significantly impacted by various types of noise from both the environment and the user's body. Noise includes unwanted components that infiltrate the data during acquisition, such as artifacts from eye movements, muscle activity, and interference from nearby electronic devices. These factors complicate the effective extraction and analysis of information, ultimately reducing the accuracy of BCI algorithms.

Several approaches exist for fine-tuning BCI algorithms, with noise filtering being a common and effective method. Noise filtering involves removing unwanted components from EEG signals while preserving essential information, thereby cleaning the signal and improving accuracy during analysis. This research examines the characteristics of several common types of noise encountered in EEG signal acquisition and evaluates the effectiveness of various denoising methods. Through testing on real signals, the report seeks to identify the optimal approach for enhancing signal quality and refining BCI algorithms

In this article, we present analysiss for evaluating EEG data through noise filtering to identify suitable methods for integrating data into BCI algorithms, with the goal of effectively developing BCI systems.

Analysis and asssessment of denoising methods for EEG Signals

Signal Evaluation Metric

To evaluate the effectiveness of denoising, the signal-to-noise ratio (SNR) can be computed both before and after the denoising process. The formula for calculating SNR is as follows:

[1] HMI lab, University of Engineering and Technology, Vietnam National Univeresity, Hanoi

[2] HMI lab, University of Engineering and Technology, Vietnam National Univeresity, Hanoi

[3] HMI lab, University of Engineering and Technology, Vietnam National Univeresity, Hanoi

[4] HMI lab, University of Engineering and Technology, Vietnam National Univeresity, Hanoi

$$SNR(Db) = 20 * log_{10} \frac{P_{signal}}{P_{noise}} \quad (1)$$

Where, P is signal energy and is calculate as following:

$$\mathrm{P} = \frac{1}{N} * \sum_{i=1}^{N} x[i]^2 \quad (2)$$

N is the number of sample and $x[i]$ is the i^{th} sample.

Wavelet Transform

Wavelet transform is a mathematical technique used to analyze signals in both time and frequency domains. This transform utilizes wavelet functions to facilitate the analysis and transformation of signals. Wavelets are signals with a finite duration and an average value of zero, meaning the total area above and below the curve of the wavelet function is zero. This characteristic makes wavelets more sensitive to local changes in the signal.

Wavelets are classified into various families based on their shapes, with each shape typically designed for effective signal analysis in a specific domain. Some common wavelet families include Haar, Daubechies, Morlet, and Mexican Hat [1]. The Morlet and Daubechies waveforms are illustrated in Figure 1. In EEG applications, the Daubechies waveform is often used for denoising due to its shape's similarity to that of the electroencephalogram signal [1].

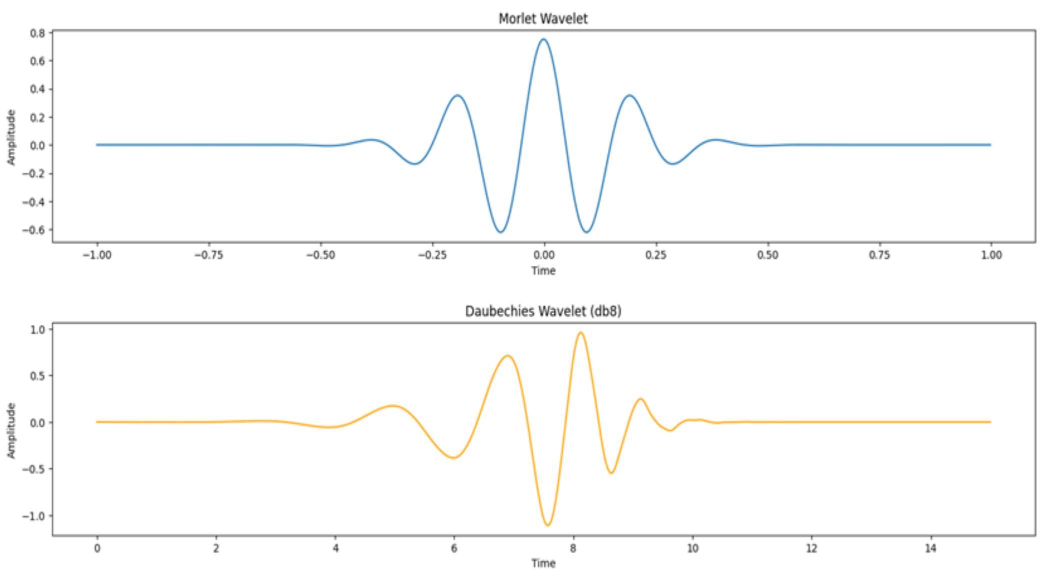

Figure 1. Wavelet waveforms: Morlet (top) và Daubechies (bottom).

The original wavelet described above is called the 'mother wavelet.' From this mother wavelet, translations in the time domain and signal dilations are applied to produce various transformed versions, referred to as 'daughter wavelets.' These daughter wavelets will be applied to the signal which are generated as follows [2]:

$$F(a,b) = \int f(t).\Psi(\frac{t-a}{b})dt \quad (3)$$

Where, a and b are the translation coefficient and dilation coefficient of the daughter wavelet, respectively, Ψ is the mother wavelet, and $F(a,b)$ is the signal when transformed at the translation coefficient a and the dilation coefficient b.

Formula (3) computes the inner product between the signal and the daughter wavelet using coefficients a and b, allowing for the assessment of similarity between the two wavelets and the analysis of the signal across different time and frequency scales.

Figure 2 illustrates the comparison the Morlet-type mother wavelet (in blue) with its variations of daughter wavelets. These signals are depicted in the time domain, where the horizontal axis represents time and the vertical axis indicates the amplitude or magnitude of the signal, demonstrating that the daughter wavelets retain the same amplitude as the mother wavelet. The stretched daughter wavelet—represented by the orange signal—has a frequency that is half that of the mother wavelet. The compressed daughter wavelet—shown in green—has a frequency that is double that of the mother wavelet. The shifted daughter wavelet—depicted in yellow—maintains the same frequency as the mother wavelet, but its position is offset by 0.5 seconds.

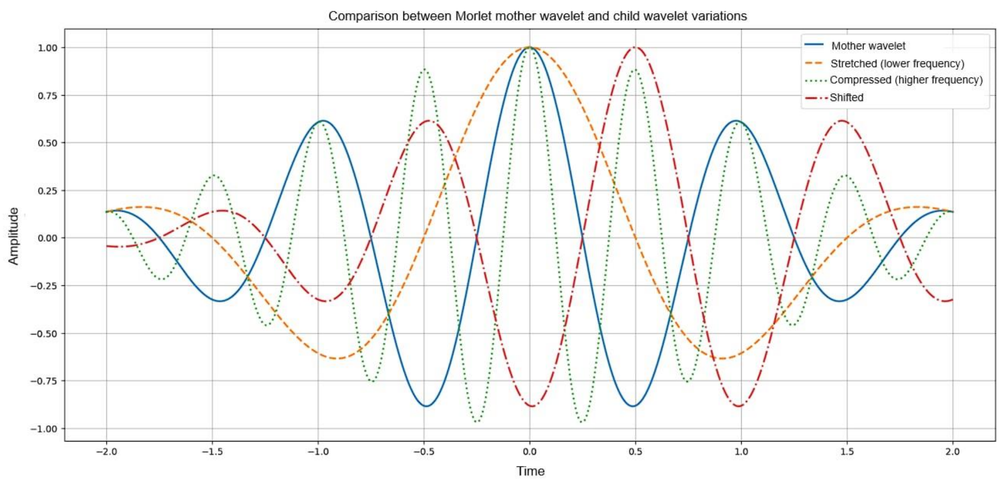

Figure 2. Daughter wavelets with different translation and dilation coefficients.

EEG signal analysis through wavelets is categorized into two types: Continuous Wavelet Transform (CWT) and Discrete Wavelet Transform (DWT). Wavelet denoising begins by selecting one of these two wavelet types for signal analysis. The mechanism of CWT closely resembles the previously described wavelet transform. In contrast, DWT decomposes the signal into ***approximation coefficients*** (which represent low-frequency information) and ***detail coefficients*** (which represent high-frequency information). These detail coefficients can be further utilized to break down the signal into coefficients with even lower frequency ranges. The main objective of DWT is to decompose the EEG signal into various frequency bands, based on the assumption that noise in the signal exhibits higher amplitudes in those bands. Thus, employing DWT serves as an effective method for filtering noise in EEG signals. Figure 3 illustrates a segment of a biological signal transformed using wavelets with two levels of decomposition.

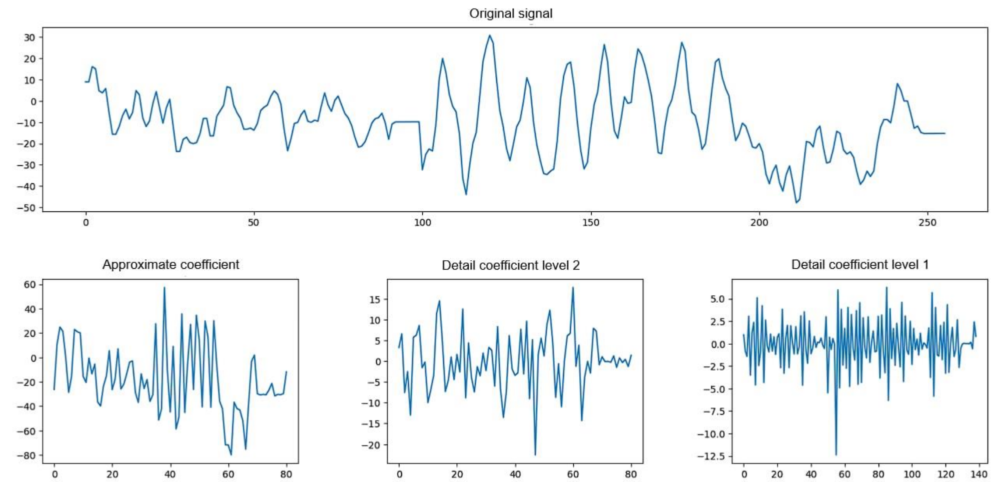

Figure 3. A segment of an EEG signal decomposed with two levels of decomposition.

The denoising process utilizing DWT involves three steps:

- ***Decomposing the signal*** into approximation and detail coefficients.

- ***Applying a threshold*** to the decomposed coefficients to remove the noise component. This threshold is calculated as follows:

$$\delta_{med} = \frac{median(|c_0|,|c_1|,...|c_{n-1}|)}{0.6745} \quad (4)$$

Where are coefficients after applying DWT, coVới c_0, c_1, ... là các hệ số sau khi biến đổi Wavelet, the value 0.6745 allows the median value to approximate the standard deviation in the case of Gaussian noise.

$$Threshold, \tau = \delta_{med}\sqrt{ln\ ln\ (N)} \quad (5)$$

N number of signal samples.

- ***Restoring the signal*** by applying the inverse Wavelet Transform. This process effectively removes noise while retaining other essential information.

Noise reduction through Wavelet Transform

The noise reduction process for the signal using Wavelet transform on a simulated signal consists of the following steps: First, generate the simulated signal, referred to as the original signal. Next, add noise to this signal to create the noisy signal. Then, apply Wavelet transform to decompose and remove the noise. Finally, compare the resulting signal with the original signal using various evaluation metrics.

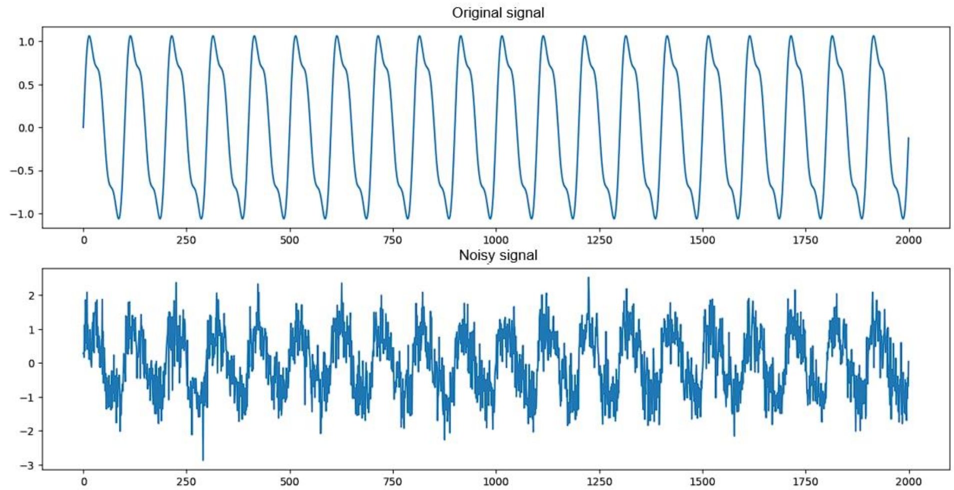

Figure 4. Original signal (top) and the signal after adding noise (bottom).

Figure 4 depicts the initial simulated EEG signal in two states: before and after the addition of noise. The original signal is simulated as a combination of sine waves at various frequencies, reflecting the characteristics of natural brain electrical activity. This signal is then added to three common types of noise:

- White Gaussian Noise (WGN): Composed of random values distributed according to a Gaussian distribution, this noise is typically evenly spread across the entire frequency range, blurring the original signal.

- Electromyography (EMG) Noise: Simulated from random values with high frequencies (> 40Hz), this noise mimics the effects of muscle activity, such as teeth grinding or jaw movements.

- Power Line Noise (PLN): Characterized by oscillations at a fixed frequency of 50Hz.

After adding the noise, the original signal becomes severely distorted, making the natural wave characteristics difficult to identify. The objective of the processing is to eliminate these noise components to restore the signal to its original condition. This not only enhances the accuracy of signal analysis but also preserves vital features within the EEG. Using the noisy signal, the Discrete Wavelet Transform (DWT) is applied to decompose it into sub-waves. Figure 5 presents the results obtained from this process, employing the 'sym12' mother wavelet at a decomposition level of 5.

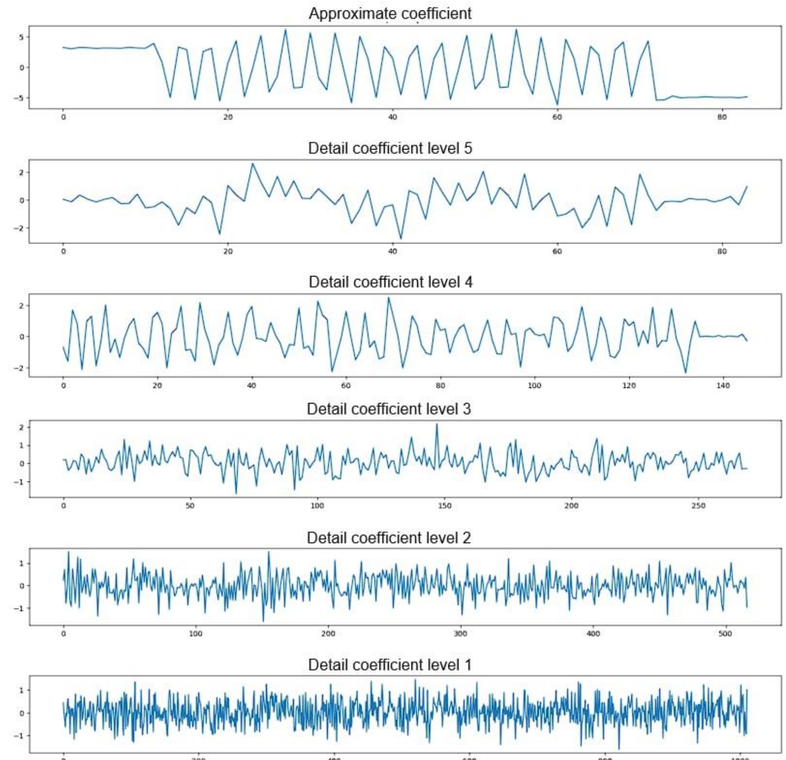

Figure 5. The coefficients obtained after using Wavelet transform.

Figure 5 illustrates the results of signal analysis, dividing it into approximation coefficients (low frequency) and detail coefficients (high frequency) using the Wavelet transform method. The approximation coefficients closely resemble the original signal, emphasizing the crucial features that must be preserved in the EEG. These coefficients exhibit low variability, making them less susceptible to high-frequency noise. In contrast, the detail coefficients consist of high-frequency components that are more significantly affected by noise. Subsequently, thresholding is applied to the signal. The coefficients resulting from this process are displayed in Figure 6, where components with values below the threshold are eliminated. After applying the threshold, it is evident that the detail coefficients remove components identified as noise. When the remaining coefficients are combined, the result is a denoised signal, as shown in Figure 7.

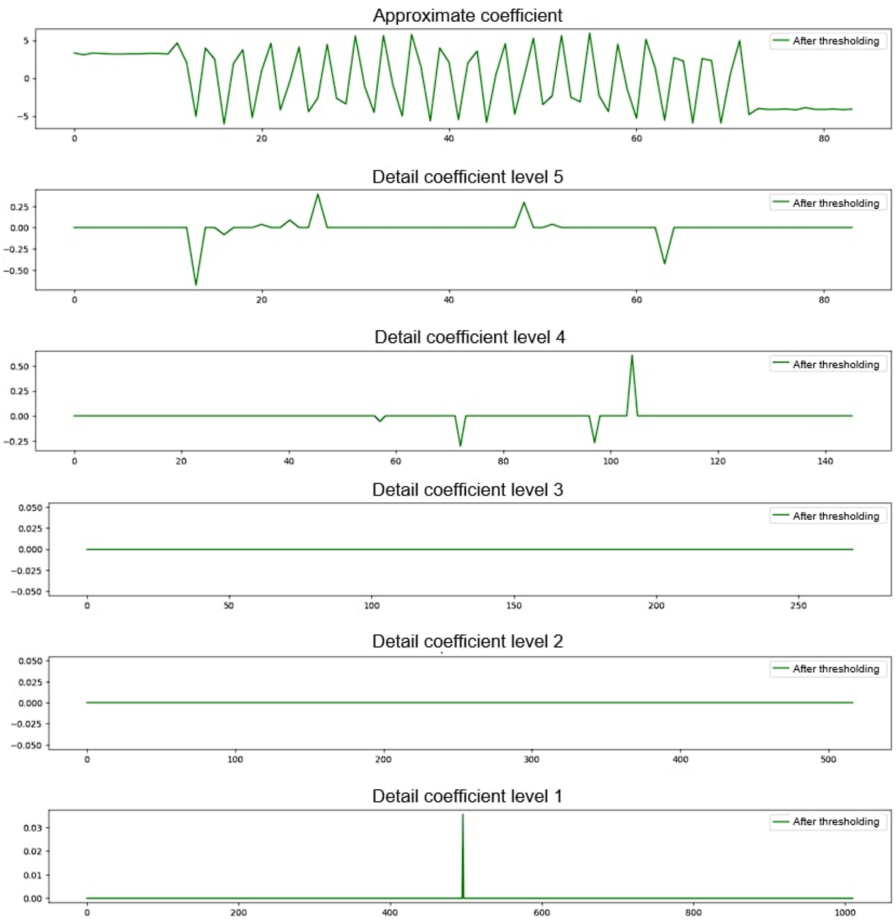

Figure 6. The coefficients obtained after using threshold.

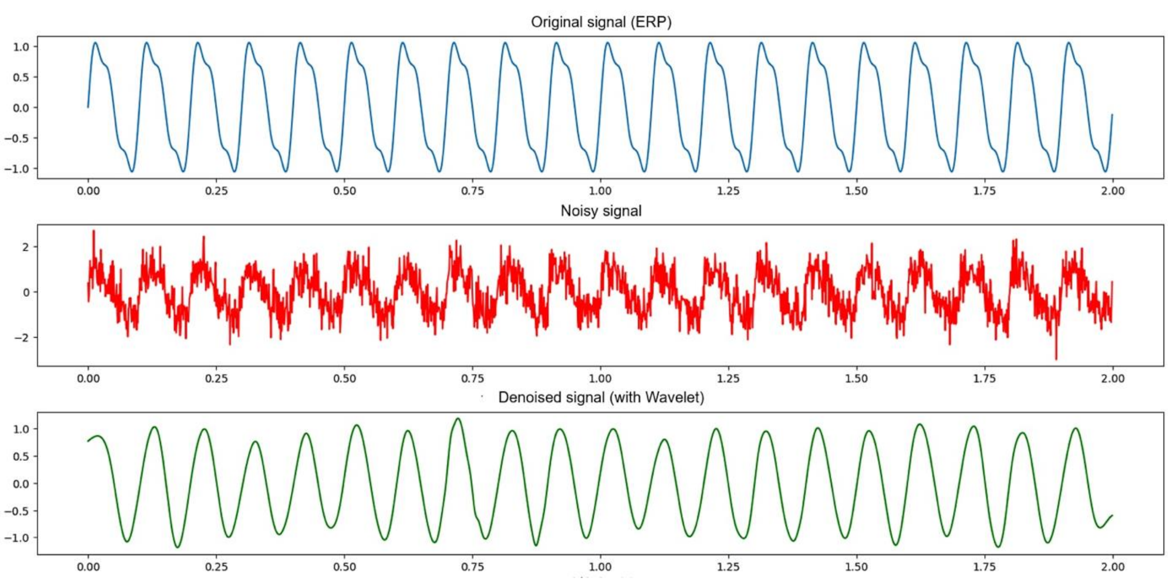

Figure 7. Denoised signal (bottom) in relation to the original signal (top) and the noisy signal (middle).

Using the SNR calculation formula, we obtain SNR of the original noisy signal is 5.02 dB while those of the denoised signal is 21.06 dB. These results clearly show that the SNR of the signal significantly improves after denoising with the Wavelet transform. The SNR value of the denoised signal is four times higher than that of the noisy signal, indicating a much cleaner signal.

Bandpass filters

Certain types of noise in EEG signals typically occur within specific frequency bands. Utilizing this characteristic, removing unnecessary frequency bands can effectively filter out unwanted noise. A bandpass filter is the ideal tool for this purpose. It is designed to allow frequencies within a specified range to pass through while blocking frequencies outside that range. A bandpass filter is defined by two key frequencies:

- ***Low cutoff frequency:*** The lowest frequency that the filter permits to pass.

- High cutoff frequency: The highest frequency that the filter permits to pass.

Common types of filters include Butterworth, Chebyshev, Bessel, and Elliptic [3] (Figure 8). The application of these filters is intended to obtain information about the ***Passband*** and ***Stopband***. Passband refers to the range of signal values that are permitted to pass through. As seen in the figure, this segment corresponds to the signal amplitude from the start until it begins to decrease (approximately at 0.3). Among the four types of filters, Butterworth offers the flattest amplitude response in the passband, consistently near 0 dB, while the Bessel response gradually declines. In contrast, Chebyshev and Elliptic filters exhibit ripples, characterized by oscillations in amplitude that increase and then decrease. Stopband denotes the range of signal values that are attenuated, corresponding to an amplitude of -∞ dB, which equates to 0 on a linear scale (indicating no signal). Interestingly, the Elliptic filter also shows ripples within the stopband.

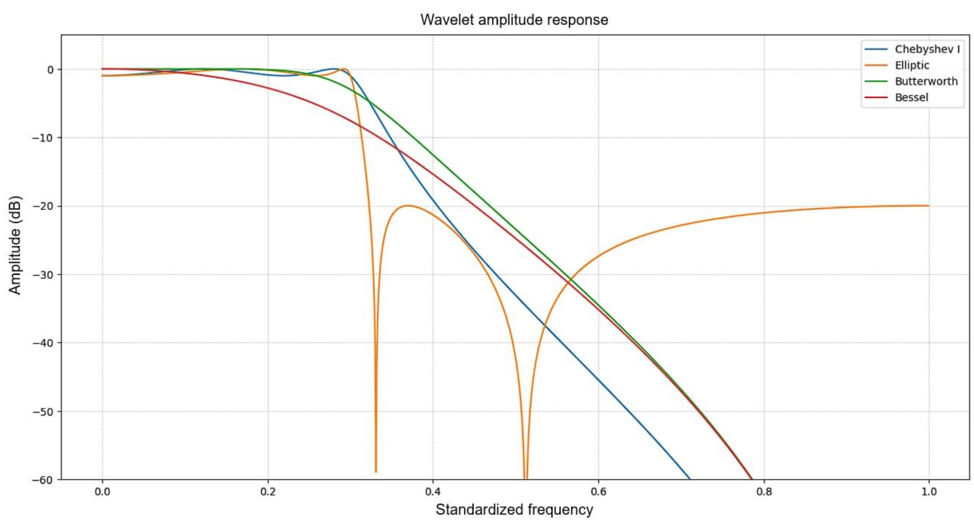

Figure 8. Amplitude response of different types of bandpass filters.

Figure 8 shows the amplitude response of various types of bandpass filters, using a normalized cutoff frequency of 0.3. The green, orange, blue and red lines indicate Butterworth, Elliptic, Chebyshev Type 1, and Bessel bandpass filters, respectively.

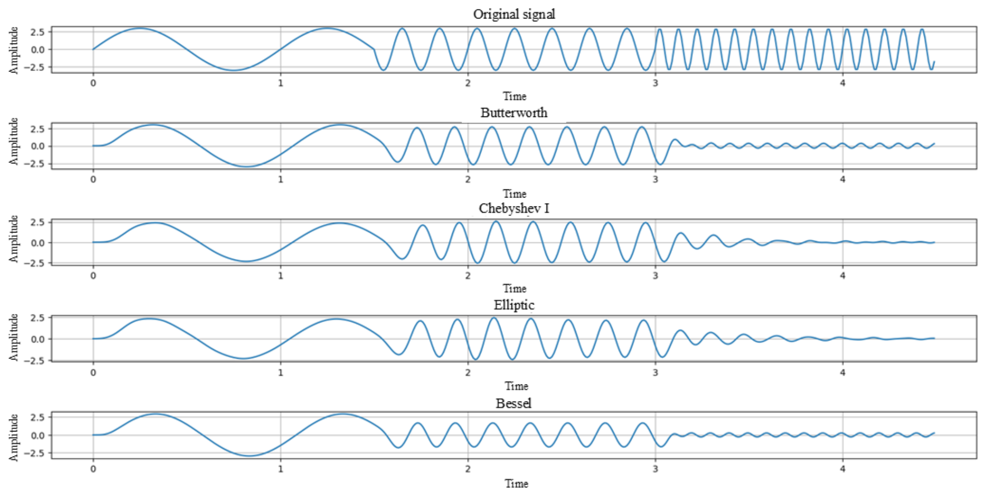

Figure 9. Comparison of the signal after passing through different bandpass filters.

Figure 9 illustrates the signal after it has passed through various types of bandpass filters with a high cutoff frequency. The original signal comprises three distinct frequency ranges, which are clearly visible at the beginning, middle, and end of the signal. Notably, in the middle segment, the amplitude of the Butterworth signal remains stable and nearly unchanged compared to the original. In contrast, the amplitudes of the Chebyshev and Elliptic signals exhibit instability, while the Bessel signal shows attenuation. In Figure 8, the signal range demonstrates amplitude attenuation as it transitions from the passband to the stopband, known as the transition band. The transition band of the Elliptic filter is the shortest, followed by Chebyshev, Butterworth, and the longest being Bessel. A longer transition band indicates that more unwanted information outside the desired frequency range may be retained. An ideal filter would have a transition band length of zero, preserving only the desired frequencies.

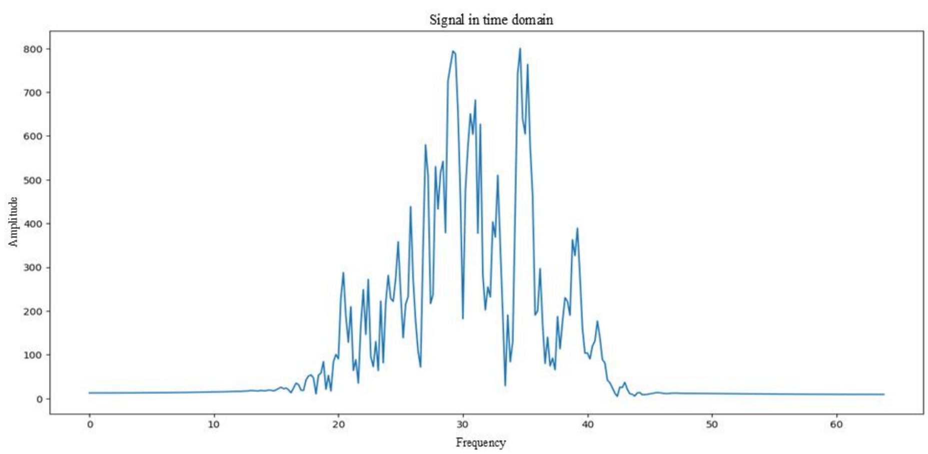

Figure 10. EEG signal after passing through a 4th-order Butterworth band-pass filter.

Figure 10 displays a segment of the EEG signal after it has passed through a 4th-order Butterworth band-pass filter (20 to 40 Hz). Some frequency components just outside the passband still persist, although their amplitudes are diminished. Besides using a fixed filter type, the order of the filter can be increased to enhance the rate of attenuation in the transition band. However, this approach will also demand additional computational resources. Based on the study and analysis of the filters mentioned above, we present a comparison of the filters in **Table 1** below.

Table 1. Comparison of some bandpass filters.

Features	Butterworth	Chebyshev	Bessel	Elliptic
Waves on the passband	No	Yes	No	Yes
Waves on the stopband	No	No	No	Yes
Attenuation rate in the transition band	Normal	Quite fast	Slow	Fast

Based on the features outlined above, it is evident that the Butterworth filter is most effective when the signal amplitude is stable and closely resembles the original signal within the passband, making it ideal for observing biological signals. Thus, in this study, we will employ a 4th-order Butterworth band-pass filter to eliminate unwanted frequency bands.

Noisy reduction using Bandpass Filters

We also simulate the EEG signal as the original signal, then introduce high-frequency noise to generate a noisy signal, which is subsequently denoised using a 4th-order Butterworth filter (Figure 11).

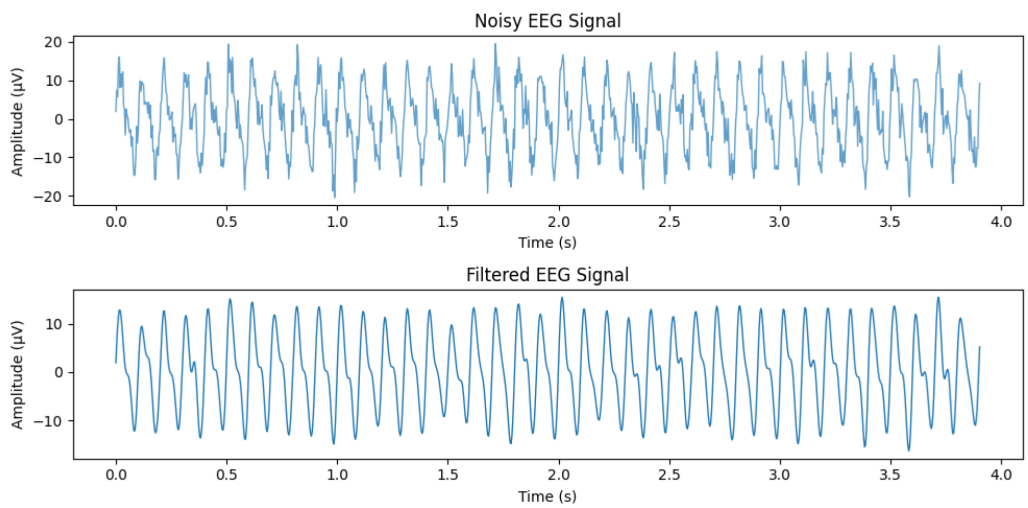

Figure 11. Denoising using a 4th-order Butterworth filter.

The SNR of the noisy signal is 17.272 dB. After denoising, it increases to 30.117 dB.

Independent Component Analysis

Independent Component Analysis (ICA) [4] is a statistical technique used to separate independent source signals from mixed observed signals. The core concept of ICA is to represent the observed signal as a sum of independent components. By applying ICA, it is possible to extract these components from the original signal, under the assumption that these sources are statistically independent and exhibit a non-Gaussian distribution. The operational diagram of ICA is shown in Figure 12. When measuring EEG signals, each channel captures not only the signal from the specific brain region it directly monitors but also includes signals from various other sources, such as noise from muscles, eyes, or even the surrounding environment. ICA operates on the premise that the observed signal X is a linear combination of the independent source signals S.

$$X = AS \tag{6}$$

Where: X and S are the matrices of signals measured from the EEG channels, signals from the independent sources to be identified (original EEG signals, noise signals caused by eye movements, etc.), respectively and A is the mixing matrix (the linear coefficients representing how the independent sources combine to form the signal X).

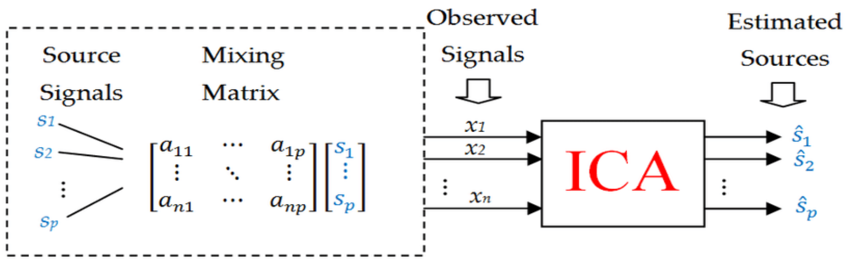

Figure 12. Block diagram of the ICA operation process [4].

After applying ICA, a matrix of components present in the input signal is produced. This enables the identification of noise components within the signal. To eliminate the noise, it is sufficient to set the coefficients of the corresponding components to zero; consequently, the reconstructed signal will no longer be affected by these noise components. ICA is particularly effective in processing noise in EEG signals because of its capability to differentiate between various types of noise, such as eye and muscular interference. For eye movement noise, ICA can identify signals caused by eye movements, which are characterized by high amplitude and low frequency. For muscle noise, ICA can separate high-frequency signals generated during muscle activity.

Noisy reduction using ICA

Figure 13 below illustrates the process of removing noise caused by blinking. The initial signal is derived from brainwave data collected from three channels: Pz, Cz, and Fz. Notably, spikes are observed on the Fz channel, corresponding to signal regions generated when the subject blinks during data collection. The noise removal process employs independent component analysis (ICA) algorithms, using the aforementioned signal channels as input, resulting in independent components as displayed in the second frame. It is noted that component number 0 (brown) exhibits characteristics similar to the noise that needs to be eliminated; thus, it is necessary to set the value of this component to zero. Finally, the signal is reconstructed from the new component signals. The restored signal image shows that the Fz channel has successfully removed the spikes caused by blinking. After noise removal, the Pz channel increased from 12.147 dB to 30.14 dB, the Cz channel rose from -1.14 dB to 32.94 dB, and the Fz channel changed from -15.04 dB to 14.30 dB.

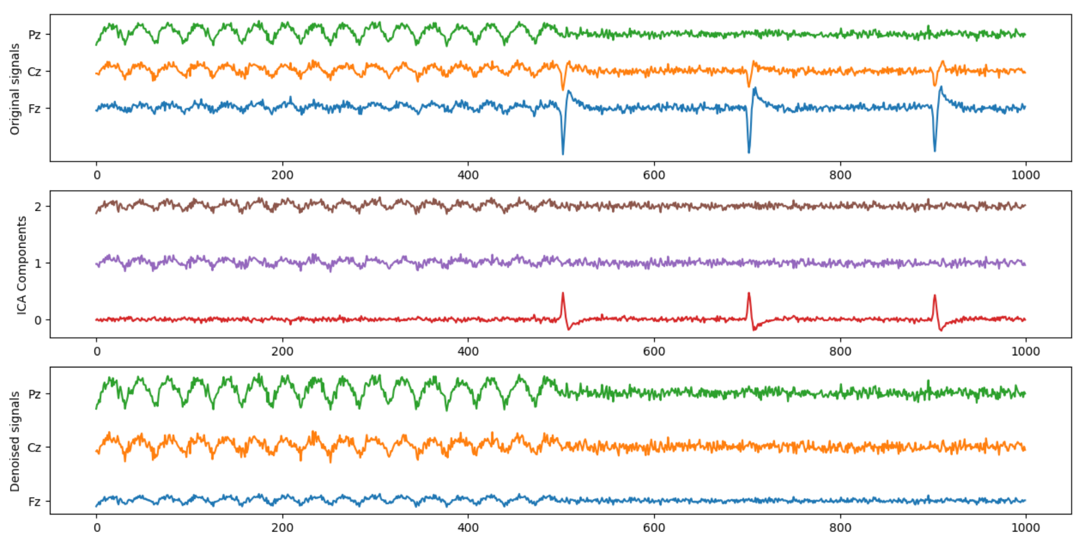

Figure 13. Applying ICA on simulated blinking noise signals.

Independent component analysis is highly effective for signals significantly affected by noise and does not rely on assumptions about the frequency or amplitude of the noise, unlike filters. However, ICA has some limitations, including the requirement for multi-channel data and high-quality signal acquisition to achieve optimal results. Unlike wavelet decomposition, which can perform noise removal on a single signal channel, ICA requires multiple signal channels to operate effectively. Additionally, using this method to remove noise necessitates expertise regarding the type of noise to accurately identify the independent components that need to be eliminated.

Various types of noise arising during EEG data acquisition

EEG signals usually have very low amplitudes, which makes them vulnerable to interference from various unwanted sources. These interferences are classified as noise, which can arise from multiple origins, including bodily activities and environmental factors. Below are some common types of noise encountered during measurements.

Noise caused by eye Movement

Noise caused by eye movement mainly arises from the activity of the muscles around the eyes during actions like blinking, gazing, or shifting gaze. The electrical potential generated in this process is commonly known as the EOG signal (electrooculogram). EOG signals typically exhibit larger amplitudes (compared to EEG signals) and are dominant in channels situated in the frontal scalp region (e.g., channels Fp1, Fp2). They primarily occur in the low-frequency range (< 8Hz), obscuring or interfering with Delta and Theta waves, which also reside within this frequency range [5].

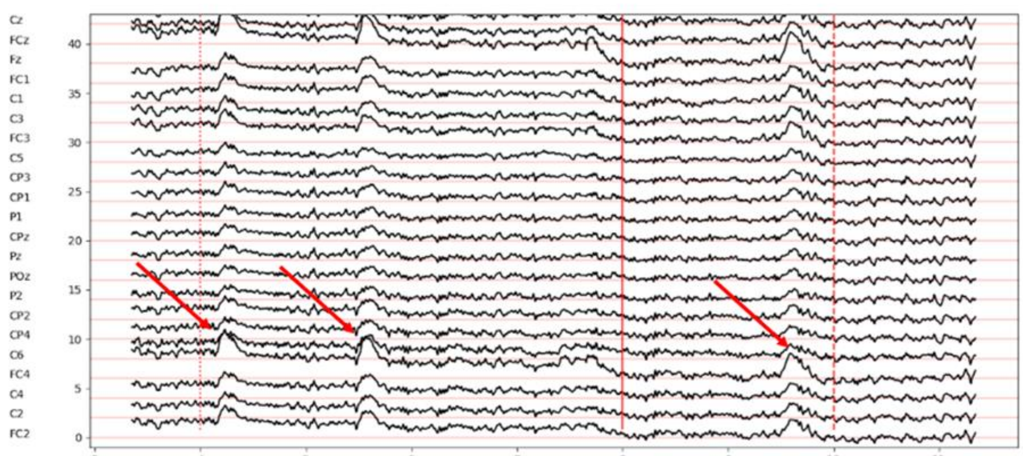

Figure 14. EOG signal.

Figure 14 above is taken from a data recording that includes eye noise. In this signal segment, eye-blink noise is evident through sudden spikes of high amplitude, while the frequency of these intervals falls below 8Hz. Since the noise originates from eye movement, the signals in the frontal channels (marked as F) are also more pronounced.

Noise caused by Mechanical Movement

Noise caused by mechanical movement arises from the activity of muscles in the head, face, or neck during EEG signal recording. Common activities include clenching teeth, muscle tension, and talking [6]. Muscle noise usually manifests in the high-frequency range with low amplitude. Upon examining the signal spectrum, muscle noise can be readily identified by the presence of discontinuous noise components concentrated in the high-frequency range.

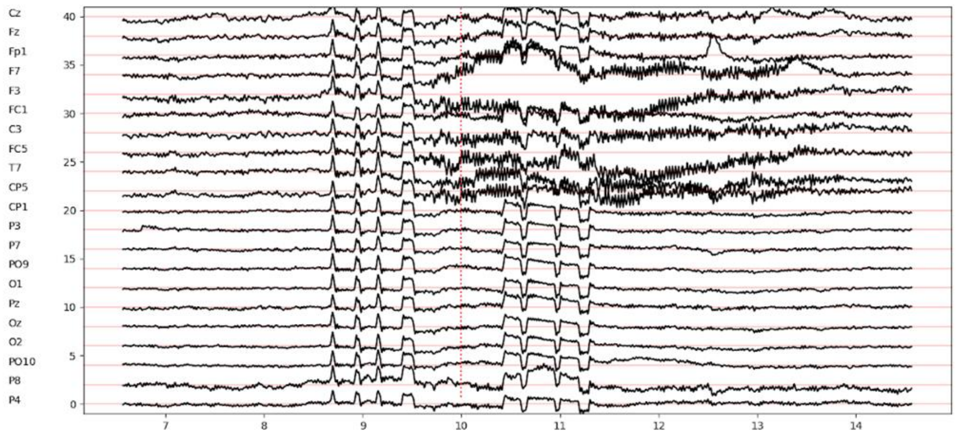

Figure 15. Muscle noise

Figure 15 presents two segments of EEG signals, clearly illustrating the presence of muscle noise. This noise is characterized by dense signal segments where oscillations become rapid and continuous for brief periods. Such patterns indicate high frequency in the EEG signal, typically arising when the muscles around the head or face are active, such as during teeth clenching, jaw movement, or muscle tension.

Noise caused by Poor Electrode Contact

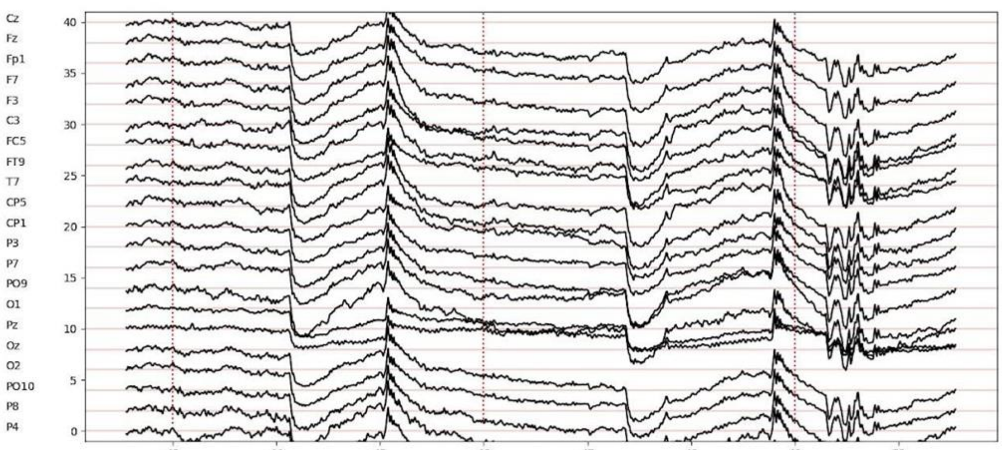

Figure 16. Noises caused by subject movement.

Noise caused by poor electrode contact occurs when the subject moves during EEG signal measurement, such as changing sitting positions or breathing heavily. These movements disrupt the contact between the electrodes and the scalp, leading to amplitude variations in the signal and potentially causing signal loss in certain channels. Moreover, specific electrodes may gradually lose contact over time due to insufficient saline solution as a conductive medium. This type of noise can manifest in one or multiple signal channels, depending on the impedance between the electrodes and the subject's scalp. When present, the amplitude can fluctuate abruptly and unpredictably, negatively impacting the quality of the signal and the accuracy of subsequent classification algorithms. Figure 16 illustrates the noise in the signal when the subject changes position during measurement, revealing significant amplitude variations across all channels, or resulting in noticeably distorted information compared to the other channels; the signals obtained during this period often become unrelated to brain activity.

Assessing the effectiveness of various denoising methods on real-world EEG signal.

EMG Denoising

Prior to denoising, the initial signal exhibits noise caused by muscle movement across several EEG channels, characterized by dense, rapid, and continuous fluctuations over a brief period (beginning at sample 500). This noise predominantly impacts the high-frequency bands (> 40 Hz), obscuring the characteristics of Gamma waves.

Figure 17. EMG denoising: original signal (top) and denoising signal (bottom).

The results of EMG denoising using ICA on a specific channel are illustrated in Figure 17. After denoising, the signal appears stabilized, with clearer waves in the desired frequency range. Undesired fluctuations have been significantly minimized without compromising the original EEG waves in the lower frequency bands. The application of ICA proves effective in removing components associated with muscle noise. When using a band-pass filter to preserve the information of the EEG signal, the filter's frequency range is typically set between 8 and 30 Hz. In these conditions, most muscle noise induced by movement is effectively eliminated. However, some instances of muscle noise may contain components with frequencies below the 30 Hz threshold, leading to a small portion of the noise persisting even after the signal passes through the filter.

EOG Signal Denoising

When analyzed, the EEG signal displays EOG segments as large spikes that recur with high amplitude and low frequency. These spikes obscure the natural characteristics of the EEG waves. Components contributing to EOG noise can be easily identified and removed using ICA. The outcomes of EOG denoising through ICA are shown in Figure 18. After denoising, the EEG waves demonstrate increased stability, with no remaining spikes from eye movement, while preserving the signal's features.

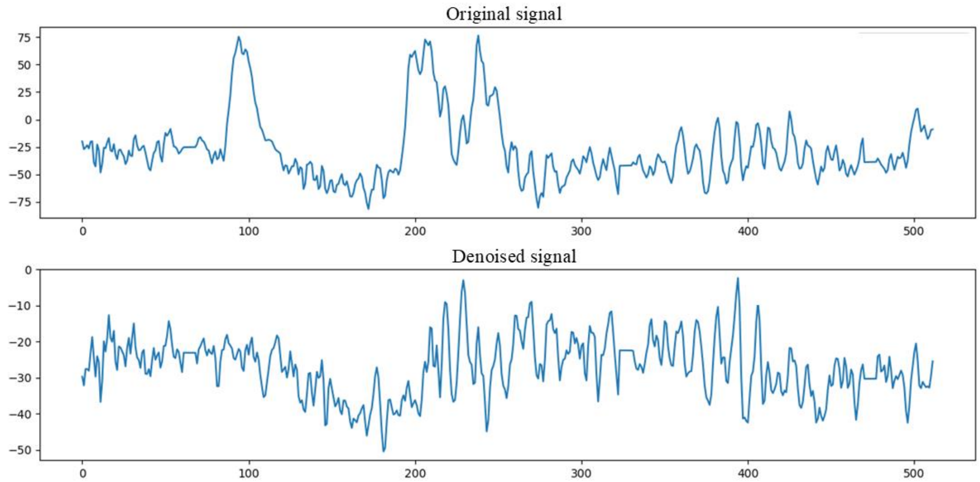

Figure 18. EOG signal denoising by ICA original signal (top) and denoising signal (bottom).

Wavelet transform is also an effective method for addressing this type of noise. The results of this approach are presented in Figure 19. With a decomposition level of 2 and the mother wavelet 'Daubechies 4', the signal after denoising has effectively eliminated the energy spikes caused by eye movements.

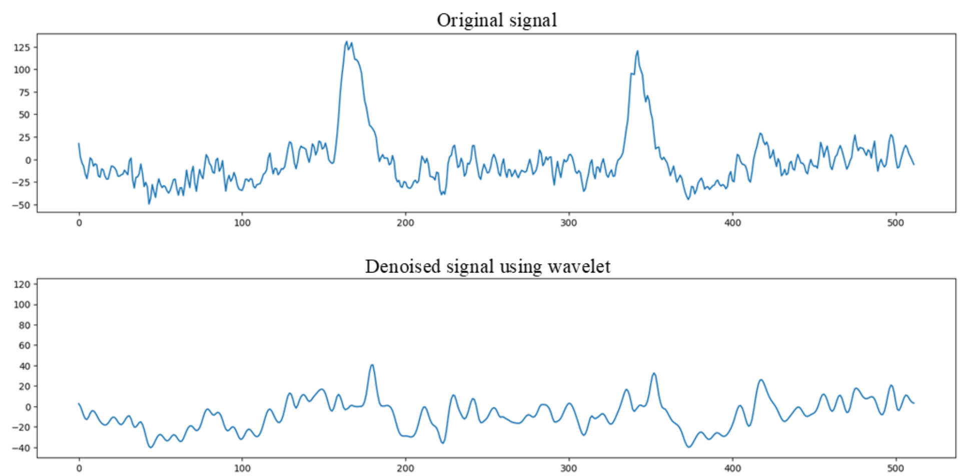

Figure 19. EOG signal denoising by wavelet transform original signal (top) and denoising signal (bottom).

Furthermore, EOG noise primarily occurs in the low-frequency range, typically below 8 Hz, and is especially prominent in the Delta frequency range (1–4 Hz). In current brain-computer interface (BCI) applications, Delta frequency information is usually not a primary focus, as it mainly reflects states such as deep sleep or less complex brain activity. Consequently, removing signals in this frequency range does not significantly impact the quality of analyses related to other frequency bands, such as Alpha (8–12 Hz) or Beta (12–30 Hz). Therefore, processing EOG noise using a high-pass filter is an effective approach. By raising the cutoff frequency, the filter can eliminate low-frequency signal information, including spikes caused by eye movements, while retaining the essential characteristics of brain waves.

Removing noise caused by Poor Electrode Contact

When poor electrode contact occurs during EEG signal acquisition, the subject should adopt a comfortable seated position and apply additional saline to ensure optimal contact between the electrodes and the scalp. This practice enhances signal quality and reduces noise. Noise from poor electrode contact can distort signals or introduce numerous abnormal data points. Band-pass filters or Wavelet techniques can effectively smooth these signals. Figure 20 shows the signal before and after it has passed through the band-pass filter. Prior to filtering, it is clear that the contact at channel FT9 is problematic, displaying an abnormal high amplitude alongside low frequency. After applying the filter, the signal becomes smoother as the low-frequency components caused by the poor connection have been eliminated.

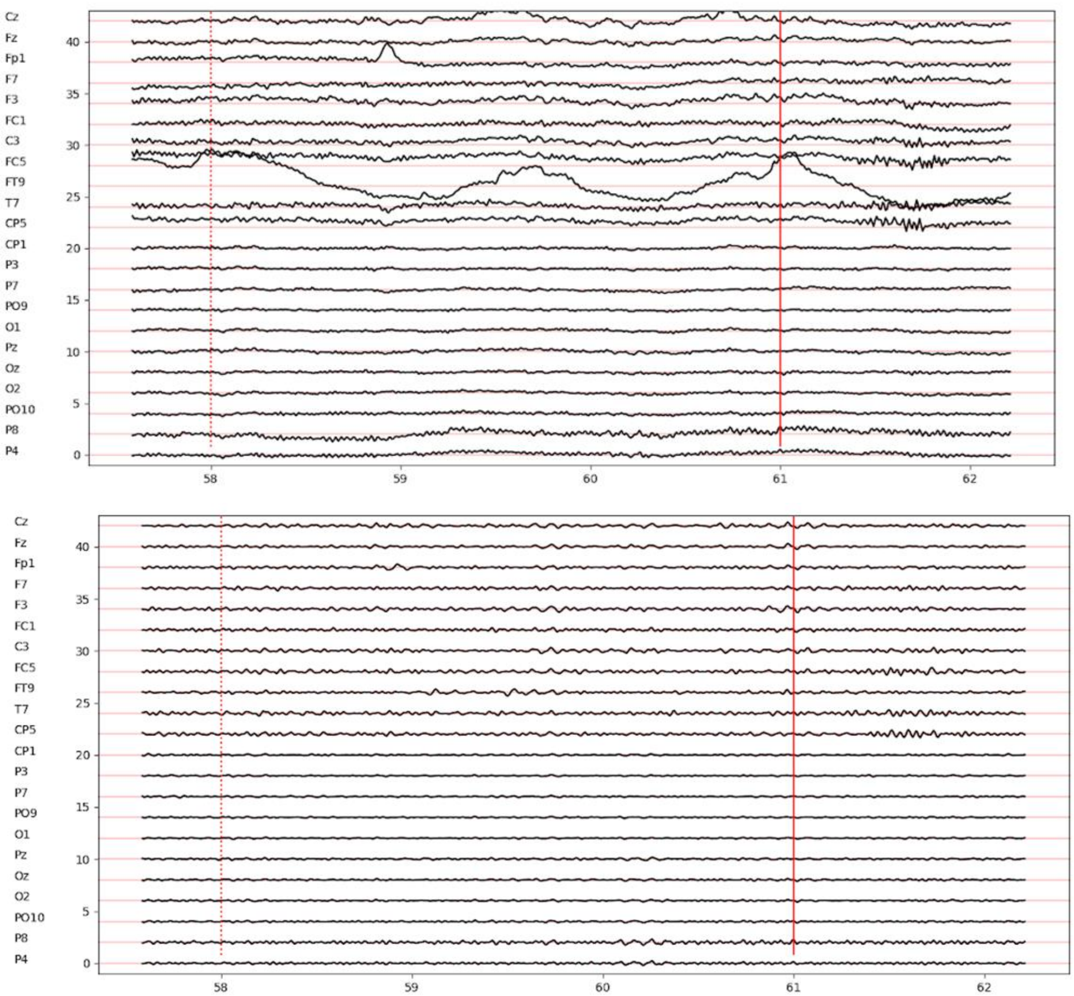

Figure 20. The signal exhibiting noise due to poor electrode contact: before (top) and after (bottom) passing through the band-pass filter

The ICA approach requires expertise from EEG analysts or physicians experienced in working with EEG waves. However, the researchers normally face challenges in accessing this specialized knowledge, which may hinder the approach's effectiveness. In contrast, the success of noise filtering through Wavelet transformation relies on various parameters selected during the denoising process, including the mother wavelet shape and threshold settings. Given that EEG waves display distinct characteristics that vary significantly among individuals, these parameters must be adjusted flexibly, introducing an additional challenge. Consequently, we considers band-pass filtering to be the most optimal method, balancing computational cost with effective automatic denoising for signal purification in BCI algorithms.

EEG signal classification after Denoising

To assess the performance of the EEG signal after denoising with the above band-pass filtering approach, we classified the denoised EEG signal and evaluated the classification performance.

Datasets

We conducted experiments using the BCI Competition IV-2a dataset [7]. Published during the 2008 competition focused on developing BCI systems, this dataset is renowned for its high quality and includes a diverse group of subjects (9 subjects), with data collected in a controlled environment using top-quality EEG equipment. As a result, it serves as an excellent foundation for theoretical performance testing of machine learning models. Additionally, the research team collected an experimental dataset (called HMIEEG) involving imagined motor imagery. Among the 72 electrode positions supported by the Emotiv EPOC Flex device, certain electrodes exhibited clearer characteristics for imagination than others. These electrodes are generally positioned near the motor cortex, the brain region responsible for planning, controlling, and executing voluntary motor tasks. Moreover, a study [8] indicated that the number of EEG signal channels could be reduced without significantly compromising signal quality and classification performance. Leveraging this insight, the research team streamlined the EEG data collection process by using only 22 electrodes arranged according to the layout shown in Figure 21 [7]. This dataset was collected with the Emotiv EPOC Flex device at a sampling frequency of 128Hz. The research team utilized these recording sessions for subjects to familiarize themselves with and calibrate the VR-BCI system and the BCI-vSpeller test, while also re-evaluating the classification performance of the models based on the EEG data collected from the team's device.

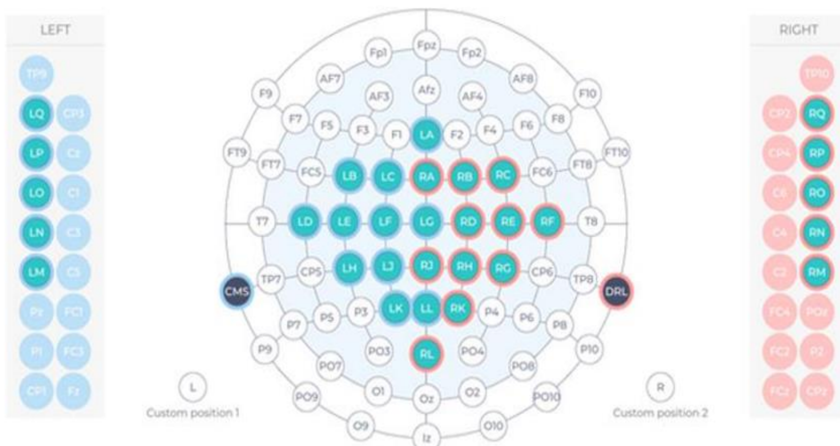

Figure 21. Electrode diagram for EEG data acquisition.

The HMIEEG experimental dataset encompasses EEG data from a single subject recorded over two sessions on different days, with each session lasting approximately 60 minutes. Each session consists of 20 trials, separated by a 20-second break. In each trial, the subject performs 12 tasks, with 3 repetitions for each task (raising the right arm, raising the left arm, raising the right leg, and raising the left leg). Before each action, the data collection system emits a notification sound. After 2 seconds, two prompt images are displayed on the computer screen for 2 seconds: one image indicating the limb to be moved (arm or leg) and an arrow showing the direction (left or right) to indicate whether the subject should move the left or right limb. The subject then engages in the corresponding imagined motor imagery task for 4 seconds.

EEG Signal Classification Performance Metric

Accuracy measures the ratio of correct predictions made by a model, calculated as:

$$Accuracy = \frac{Correct\ predictions}{Total\ cases} \qquad (7)$$

However, accuracy alone does not provide insights into the classification of individual classes, such as which class is most accurately classified or which class experiences the most misclassification.

Cohen's kappa coefficient is a widely used statistical measure for assessing agreement between two raters, particularly for imbalanced datasets. Unlike accuracy, Cohen's kappa accounts for class distribution imbalances and is calculated using a confusion matrix as follows:

$$\kappa = \frac{p_0 - p_e}{1 - p_e} \quad (8)$$

Where: p_0 is the overall accuracy of the model, and p_e is the frequency of agreement between the model's predictions and the true class values.

We utilized the BCI Competition IV-2a dataset and the HMIEEG dataset to evaluate the performance of the LDA algorithm [9] using CSP features [10] across four different parameter sets, labeled A, B, C, and D, as detailed in Table 2. The training results from the BCI Competition IV-2a dataset were assessed based on Accuracy and K-score, as presented in Table 3.

Table 2. Diffirent dataset parameter sets

Parameter sets	**MI taskes**	**Signal window (s)**	**Bandpass filter (Hz)**
A	Left hand – Right hand	2.5 - 3.5	8 - 15
B	Left hand – Right hand	2.5 - 4.5	8 - 15
C	Right hand – leg	2.5 - 3.5	8 - 15
D	Right hand – leg	2.5 - 3.5	8 - 30

Table 3. LDA algorithm performance on BCI IV-2a dataset

Subjects	**A**		**B**		**C**		**D**	
	Acc	**K-score**	**Acc**	**K-score**	**Acc**	**K-score**	**Acc**	**K-score**
1	96.45	0.9291	80.85	0.6167	71.94	0.4403	93.53	0.8706
2	38.03	-0.2394	39.44	-0.2113	97.14	0.9429	98.57	0.9714
3	91.97	0.8393	99.27	0.9854	94.93	0.8984	88.41	0.7688
4	59.48	0.194	99.14	0.9828	81.9	0.6355	83.62	0.6742
5	71.85	0.4424	91.85	0.8358	86.13	0.7242	99.27	0.9854
6	78.7	0.5726	100	1	99.08	0.9817	100	1
7	66.43	0.3242	95.71	0.9142	93.57	0.8714	99.29	0.9857
8	80.6	0.6137	99.25	0.9851	92.7	0.8539	82.48	0.6487
9	63.08	0.4374	100	1	76.12	0.5287	94.03	0.8805
Avg	**71.83**	**0.4374**	**89.5**	**0.7898**	**89.04**	**0.7814**	**93.24**	**0.865**

In Table 3, parameter set B utilizes a larger signal window than parameter set A, resulting in more EEG data and a higher average classification outcome. However, for some subjects, the distinction in EEG signals between the imagined motor imagery tasks for the left and right hands is not clear, which leads to poor classification performance. Furthermore, employing a signal window longer than 2 seconds decreases the usability of the BCI system, resulting in extended sessions for patients. Consequently, during testing with parameter sets C and D, the team adopted a 1-second signal window, varying the imagined motor imagery tasks and adjusting the bandpass filter. In parameter set C, the team compared the tasks for the right hand and leg, using the same bandpass filter as in parameter sets A and B. Although the average classification result showed a slight decrease compared to parameter set B, it remained consistent and stable across all 9 subjects, with none achieving a performance below 50%. To provide additional data for the classification algorithm, parameter set

D incorporated a wider bandpass filter (8–30 Hz), which yielded the best classification results in terms of both Accuracy and average K-score. We then selected and applied the signal window and bandpass filter parameters from set D to test the LDA algorithm on the HMIEEG experimental dataset. The classification results are presented in Table 4 below.

Table 4. LDA algorithm performance on HMIEEG dataset

MI taskes	Accuracy	K-score
Left hand - leg	89.04	0.7814
Right hand – leg	82.19	0.6455
Left hand – Right hand	100	1

The experiments demonstrated that the denoised signals achieved high performance and hold significant potential for the implementation of BCI applications.

CONCLUSION

In this article, we examined several common errors encountered during the acquisition of EEG signals. We also analyzed various noise processing approaches suitable for EEG data. Independent Component Analysis (ICA) is effective for high-level noise filtering; however, it requires expert knowledge to identify and remove noise components, making it less suitable for automatic noise filtering. The effectiveness of Discrete Wavelet Transform (DWT) in noise filtering depends on the choice of the mother wavelet, decomposition level, and threshold selection. Bandpass filters necessitate defining the frequency range of signals to ensure effective noise reduction while preserving EEG signal information, providing stable filtering that can eliminate most noise at a low cost.

Additionally, we applied a bandpass filter to denoise the signals prior to classification for BCI application implementation. Experiments demonstrated high classification performance when the bandpass filter was used for denoising.

REFERENCES

Mamun, Md, Mahmoud Al-Kadi, and Mohd Marufuzzaman. "Effectiveness of Wavelet denoising on electroencephalogram signals." Journal of applied research and technology 11.1 (2013): 156-160. doi: 10.1016/S1665-6423(13)71524-4.

Burrus, Charles & Gopinath, R. & Guo, H.. (1998). Introduction to Wavelets and Wavelet Transform—A Primer. Recherche. 67.

Li Tan. Digital Signal Processing Fundamentals and Applications (3rd Edition). Academic press. ISBN: 978-0-12-374090-8. 2018.

Mika, Dariusz, Grzegorz Budzik, and Jerzy Jozwik. "Single channel source separation with ICA-based time-frequency decomposition." Sensors 20.7 (2020): 2019. doi: 10.3390/s20072019.

Bhandari, Ayush, et al. "Wavelet based compression technique of Electro-oculogram signals." 3rd Kuala Lumpur International Conference on Biomedical Engineering 2006: Biomed 2006, 11–14 December 2006 Kuala Lumpur, Malaysia. Springer Berlin Heidelberg, 2007. doi: 10.1007/978-3-540-68017-8_111.

Goncharova, Irina I., et al. "EMG contamination of EEG: spectral and topographical characteristics." Clinical neurophysiology 114.9 (2003): 1580-1593. doi: 10.1016/S1388-2457(03)00093-2.

C. Brunner et al., "BCI Competition 2008–Graz data set A," Institute for knowledge discovery (laboratory of brain-computer interfaces), Graz University of Technology, vol. 16, pp. 1-6, 2008.

Altaheri H, Muhammad G, Alsulaiman M, Amin SU, Altuwaijri GA, Abdul W, Bencherif MA, Faisal M. Deep learning techniques for classification of electroencephalogram (EEG) motor imagery (MI) signals: A review. Neural Computing and Applications. 2023 Jul;35(20):14681-722. doi: 10.1007/s00521-021-06352-5.

Fisher, Ronald A. "The use of multiple measurements in taxonomic problems." Annals of eugenics 7.2 (1936): 179-188. doi: 10.1111/j.1469-1809.1936.tb02137.x.

Ramoser, Herbert, Johannes Muller-Gerking, and Gert Pfurtscheller. "Optimal spatial filtering of single trial EEG during imagined hand movement." IEEE transactions on rehabilitation engineering 8.4 (2000): 441-446. doi: 10.1109/86.895946.